JACS
JOURNAL OF THE AMERICAN CHEMICAL SOCIETY
Communication
pubs.acs.org/JACS

Evaporation-Induced Buckling and Fission of Microscale Droplet Interface Bilayers

Jonathan B. Boreyko,[†] Prachya Mruetusatorn,[§] Stephen A. Sarles,[⊥] Scott T. Retterer,[†,‡] and C. Patrick Collier*[,†]

[†]Center for Nanophase Materials Sciences and [‡]Biological and Nanoscale Systems Group, Oak Ridge National Laboratory, Oak Ridge, Tennessee 37831, United States

[§]Department of Biosystems Engineering & Soil Science and [⊥]Department of Mechanical, Aerospace, and Biomedical Engineering, The University of Tennessee, Knoxville, Tennessee 37996, United States

Supporting Information

ABSTRACT: Droplet interface bilayers (DIBs) are a robust platform for studying synthetic cellular membranes; however, to date no DIBs have been produced at cellular length scales. Here, we create microscale droplet interface bilayers (μDIBs) at the interface between aqueous femtoliter-volume droplets within an oil-filled microfluidic channel. The uniquely large area-to-volume ratio of the droplets results in strong evaporation effects, causing the system to transition through three distinct regimes. First, the two adjacent droplets shrink into the shape of a single spherical droplet, where an augmented lipid bilayer partitions two hemispherical volumes. In the second regime, the combined effects of the shrinking monolayers and growing bilayer force the confined bilayer to buckle to conserve its mass. Finally, at a critical bending moment, the buckling bilayer fissions a vesicle to regulate its shape and mass. The μDIBs produced here enable evaporation-induced bilayer dynamics reminiscent of endo- and exocytosis in cells.

Synthetic lipid bilayers are useful models of cellular membranes. Traditionally, synthetic membranes were produced in the form of planar lipid bilayers exhibiting fixed size and shape, which enabled the controlled analysis of transport phenomena and electrophysiology.[1] In nature, cellular and intracellular membranes are dynamic systems that experience continual deformation and can even undergo fusion and/or fission, for example during endo- and exocytosis.[2] This dynamic behavior has been observed in lipid vesicles[3] that were prepared and manipulated to control and observe budding, fusion, and fission.[4] Mechanisms for the dynamic response of these vesicle membranes included osmotic (or temperature-driven) deflation,[4a,5] interactions with salts,[4b] proteins,[4c,6] lipids,[4d] or peptides,[4f,7] and localized wetting by aqueous compartments.[4g,h,8] Recently, the shape change of supported planar bilayers was also characterized by straining the supporting interface[9] or by inserting additional biomolecules into the membrane.[10]

Despite all of the recent progress concerning the dynamic morphology of vesicles and supported planar bilayers, relatively little is known concerning the dynamics of suspended planar membranes. Suspended planar bilayers have the dual benefit of allowing control of the biochemistry on either side (unlike vesicles), while their enhanced fluidity enables large deformations (unlike supported planar bilayers). These features were exploited to fission giant vesicles ($D \approx 300$ μm) from a suspended planar bilayer via an impinging fluid jet.[11] The most common technique for creating such membranes is to suspend the bilayer across an aperture opened in a solid wall.[1,11] This has only recently become practical at cellular length scales using microfluidic channels.[12] A promising new technique for creating fluid bilayers is to form a liquid-supported bilayer between adjacent water droplets immersed in oil and exhibiting lipid monolayer interfaces,[13a] commonly referred to as a droplet interface bilayer (DIB).[13b] So far, most DIBs have relied on the manual positioning of millimetric droplets using a micropipet,[13] electrodes,[14] or lasers.[15] While DIBs have also been assembled in microfluidic chips using dielectrophoresis,[16] electrowetting on dielectric (EWOD),[17] thin tubes,[18] or flow focusing,[19] none have obtained droplets smaller than $D \approx 200$ μm. Furthermore, the dynamic response of DIBs to the evaporation of the droplets has not been characterized.

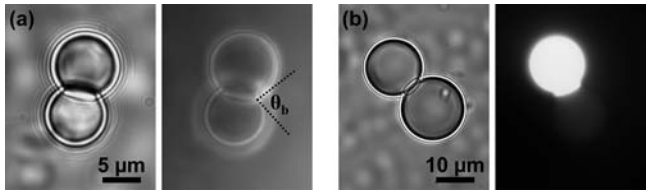

Figure 1. μDIBs formed in an oil microchannel with 2 mM DOPC lipid. (a) Bright-field and fluorescent imaging of μDIBs containing fluorescently tagged lipids. (b) Bright-field and fluorescent imaging with fluorescein in one droplet.

Here, we generate microscale droplet interface bilayers (μDIBs) by bringing together femtoliter-volume droplets in a lipid−oil microchannel. The 5−10 μm initial diameters of the droplets results in uniquely large area-to-volume ratios of ~1 μm^{-1}, 2 orders of magnitude larger than with previous DIBs. This results in dramatic evaporation effects that passively reveal the dynamics of μDIBs undergoing shape change. The energetic favorability of the formed bilayer coupled with the evaporation of

Received: February 22, 2013
Published: April 3, 2013

   dx.doi.org/10.1021/ja4019435 | J. Am. Chem. Soc. 2013, 135, 5545−5548

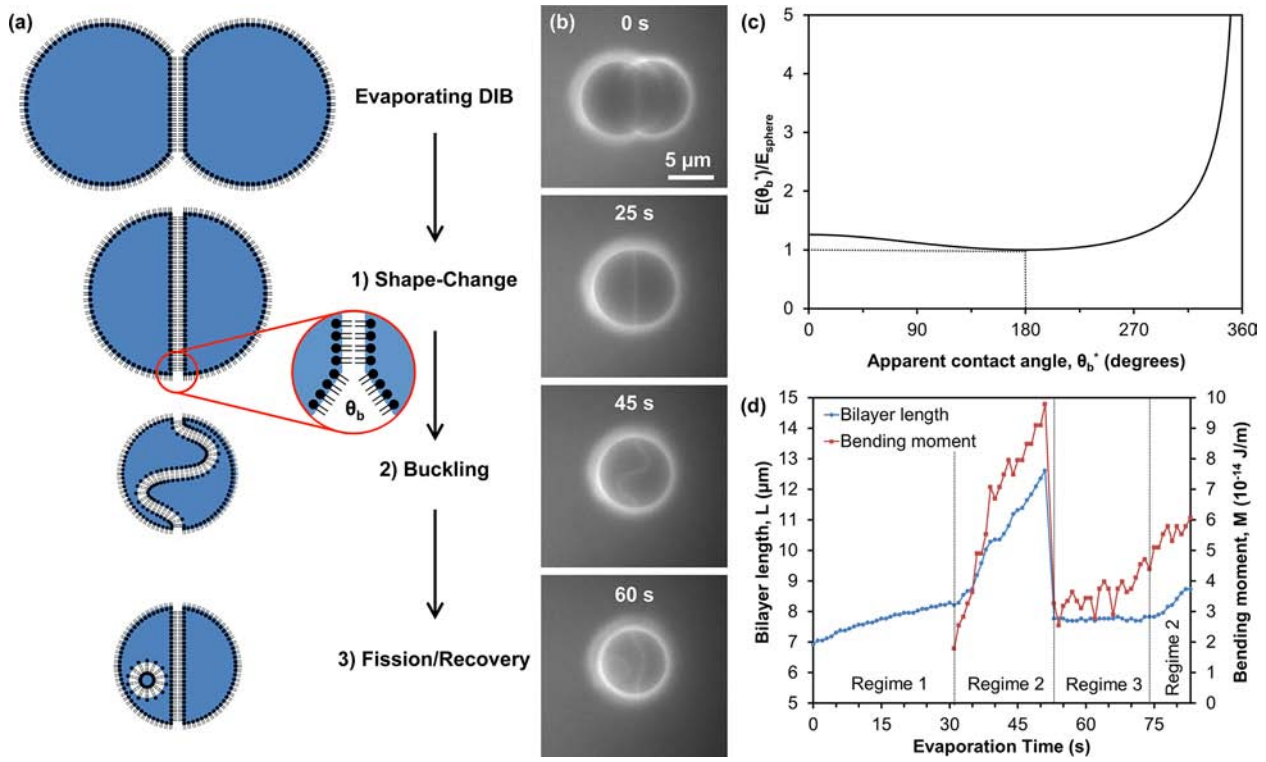

Figure 2. (a) Schematic and (b) fluorescent imaging of the progressing regimes of an evaporating μDIB. (c) The droplets shrink to a spherical shape (θ_b* = 180°) to minimize the surface energy of the monolayer interfaces. (d) The cross-sectional length of the bilayer is continuously fed by lipids from the shrinking monolayers, resulting in buckling and eventually fission at a critical bending moment.

the droplets forces a "conveyor-belt" effect, where lipids in the shrinking monolayer interfaces are forced to pair together and slide into the growing bilayer area to conserve their mass. This transformation culminates in the confinement, buckling, and fission of the lipid bilayer.

Femtoliter droplets were generated and joined together in a lipid−oil microchannel by applying timed pressure pulses to opposing side channels filled with deionized water.[20] Droplet formation was enabled by the abrupt change in height from the side-channels to the larger central channel, resulting in shape-induced pinch-off upon actuation.[21] When 2 mM 1,2-dioleoyl-*sn*-glycero-3-phosphocholine (DOPC) lipid is mixed into the purified soybean oil used in the central channel, two water droplets form a μDIB upon contact instead of coalescing together (Figure 1). The presence of the outer lipid monolayers and inner lipid bilayer were confirmed by fluorescently labeling DOPC with 0.1 mol % 1,2-dipalmitoyl-*sn*-glycero-3-phosphoethanolamine-*N*-(lissamine rhodamine B sulfonyl), ammonium salt (Figure 1a). The lipid bilayer was also identified by selectively adding 250 μM fluorescein into one of the two side channels now containing a Tris buffer solution (pH 8.0), revealing the sharp contrast in fluorescent signal across the bilayer between the droplets (Figure 1b). It has been previously shown that fluorescein can leak across DIBs without the aid of ion channels,[18] but this was not observed here due to the dominance of the evaporative time scale (minutes) over the leakage time scale (hours).

The equilibrium contact angle of DIBs (θ_b) is defined by a balance of the monolayer surface tension (γ_m) and bilayer surface tension (γ_b) vectors at the three-phase contact line:[15b]

$$2\cos(\theta_b/2) = \gamma_b/\gamma_m \quad (1)$$

Here, $\theta_b = 85° \pm 3°$ for DIBs formed with pure water droplets (Figure 1a), comparable to a previous report.[15b] To ensure that evaporation effects did not affect the measured contact angle, the surrounding poly(dimethylsiloxane) (PDMS) chip was soaked in water overnight to minimize the droplet shrinkage rate (~10 μm^2/min), and an image was captured immediately after the μDIB attained a steady-state shape. The surface tension of the lipid monolayer interfaces was measured to be $\gamma_m = 15.9 \pm 0.3$ mN/m using a goniometer (see Supporting Information). Therefore, the surface tension of the bilayer interface is calculated to be $\gamma_b = 23.4 \pm 1.0$ mN/m. The smaller value of θ_b in Figure 1b is due to the Tris buffer solution altering the surface tension values.

The dynamics of evaporating μDIBs were observed and characterized (Figure 2). A dry PDMS chip was utilized to increase the shrinkage rate by an order of magnitude (~100 μm^2/min),[20b] resulting in droplet lifetimes of ~3 min. Any shrinkage of the bilayer area during evaporation would necessitate either unzipping or compressing the bilayer. Unzipping would disrupt the attractive interactions between the hydrophobic tails. In addition, lipid bilayers are known to be relatively incompressible.[22] Therefore, the lipids in the bilayer are preserved while the outer monolayer areas preferentially shrink, creating three distinct regimes during evaporation (Figure 2a,b) which are detailed below.

Regime 1: Shape-Change. As the droplets begin to evaporate, the energetic unfavorability of the bilayer decreasing its area causes the two droplets to morph into hemispheres, such that the system now resembles a single spherical droplet ($\theta_b \rightarrow$ 180°). Interestingly, the area of the bilayer interface did not remain constant during droplet shrinkage and shape-change, but rather continuously increased from 38 to 54 μm^2 (as estimated by its cross-sectional diameter). This growth is due to the

dx.doi.org/10.1021/ja4019435 | J. Am. Chem. Soc. 2013, 135, 5545−5548

diminishing surface area of the monolayers, which forces some lipids from each monolayer to pair together as they slide onto the ends of the bilayer, analogous to items on conveyor belts.

The shape-change of the droplets raises an apparent dilemma: the three-phase line still appears to be in equilibrium, yet the γ_b vector should vanish as θ_b reaches 180° (eq 1). A recent report on DIBs also observed transformation into a spherical shape during the evaporation of chloroform in the continuous phase, attributing this to the values of γ_m and γ_b approaching zero as the composition of the organic phase was continuously tuned.[19] Here, the composition of the organic phase was unchanged throughout all experiments. There are three possible explanations for the shape-change, none of which are mutually exclusive:

(i) While the *apparent* contact angle (θ_b*) of the bilayer has increased to 180° to accommodate the preferential shrinkage of the monolayer interfaces, it is possible the intrinsic contact angle (θ_b) at the three-phase line is at an equilibrium value smaller than 180° (inset in Figure 2a). In some systems, the apparent contact angle observed by an optical microscope can be dramatically different from the intrinsic contact angle made at the three-phase line on the molecular level, for example with drops on superhydrophobic surfaces.[23] Localized curvature at the three-phase line also seems likely here, as an intrinsic angle of $\theta_b = 180°$ would mandate perfectly sharp corners between the monolayers and bilayer.

(ii) In addition to lipids in the shrinking monolayer transferring to the growing bilayer, lipid compression could also be occurring during evaporation. This would alter the values of γ_m and/or γ_b and therefore change the equilibrium value of θ_b. The area lost by both monolayers during shape-change was about 34 μm^2 each, approximately twice as large as the 16 μm^2 gained by the bilayer area. Therefore roughly 36 μm^2 of the evaporated area in the monolayers (~10% of the total monolayer area) cannot be readily accounted for by growth in the bilayer area. This suggests that the packing density of the lipids could be increasing. It has been previously reported that increasing the packing density of lipid monolayers[24] and bilayers[25] can decrease their surface tension and cause fluctuations, buckling, and fission.

(iii) Finally, a nonequilibrium steady state is also possible, where the unbalanced three-phase line exhibits a net receding force but is being continually replenished by the growing bilayer.

Regime 2: Bilayer Buckling. Once the droplets finish morphing into the shape of a single sphere, the apparent contact angle remains at $\theta_b* = 180°$ as the system continues to evaporate. This is due to the spherical shape of the system minimizing the area and surface energy of the lipid monolayer interfaces. For any given volume of water, the difference in the overall surface energy for any apparent contact angle θ_b* compared to the spherical shape of $\theta_b* = 180°$ is given by the geometric relation:

$$\frac{E(\theta_b{}^*)}{E_{sphere}} = (1 - \cos\theta)\left(\frac{(2 + \cos\theta)(1 - \cos\theta)^2}{2}\right)^{-2/3} \quad (2)$$

where $\theta = (2\pi - \theta_b*)/2$ (see Supporting Information). It can be seen that the surface energy reaches a global minimum at $\theta_b* = 180°$ and becomes particularly unfavorable for contact angles $\theta_b* > 180°$ (Figure 2c). Equation 2 explains why the system remains spherical throughout rather than continuing to deform to the nonfavorable shape of a convex lens.

The fixed spherical shape of the system results in a confined bilayer as evaporation continues. The outer monolayer areas are shrinking while the bilayer area continues to grow due to the "conveyor-belt" effect described in Regime 1. Because lipid bilayers are relatively incompressible compared to their low bending stiffness,[22] the bilayer buckles into an increasingly curved shape as it becomes confined. In most trials the buckling bilayer assumed a sinusoidal shape; however, single-mode buckling was also observed in a minority of droplets. The transition temperature of DOPC is −20 °C, well below the experimental temperature of 25 °C, therefore the lipids in the buckling bilayer are expected to be in the liquid phase. Upon initiation of buckling, the bilayer undulated with amplitudes of ~1 μm. This flickering effect could be due to fluctuations in the curvature and localized stress of the buckling bilayer or to thermal fluctuations[22a] triggered by a decrease in surface tension.[25] Previous reports have observed buckling for lipid tubules trapped inside of evaporating liquid droplets on a glass substrate[26] and induced shape change[27] and fission[28] in lipid bilayers by subjecting them to shear stress.

Regime 3: Fission/Recovery. As the buckling bilayer becomes increasingly confined, its radius of curvature gradually decreases toward a critical value (R_C) where fission occurs. The critical bending moment required for fission (M_C) can be estimated by measuring R_C and using the known bending stiffness of phospholipid bilayers ($\kappa \approx 10 k_b T$):[22a,29]

$$M_C \approx 2\kappa/R_C \quad (3)$$

The value of M_C corresponds to deforming the buckling protrusion(s) beyond a hemispherical shape, at which point shape-induced shear can pinch off a vesicle. The degree of deformation required for vesicle pinch-off can be quantified using the Capillary number:[30]

$$Ca \approx \frac{H_C - 2R_C}{H_C + 2R_C} \quad (4)$$

where H_C is the total height of a protrusion in the buckling bilayer. The values of R_C and H_C were measured for six different evaporating μDIBs of similar size ($L_C = 12 \pm 1$ μm) to calculate the critical bending moment and Capillary number required for fission (Table 1). The critical value of $Ca = 0.25 \pm 0.1$ is equivalent to the deformation required to pinch off a water droplet from a pressurized microfluidic channel into an oil reservoir.[31]

Table 1. Critical Values of a Buckling Bilayer at Fission

trial	R_C (μm)	H_C (μm)	M_C (10^{-14} J/m)	Ca
1	0.84	3.0	9.8	0.29
2	0.84	2.4	9.8	0.17
3	0.84	3.2	9.8	0.31
4	0.91	2.9	9.1	0.23
5	1.04	3.2	8.0	0.21
6	0.78	2.8	10.6	0.28
avg	0.87	2.9	9.5	0.25
$\pm 2\sigma$	±0.18	±0.6	±1.8	±0.10

The rupture of the buckling bilayer served to rectify its shape and bending moment (Figure 2d). Rupture resulted in the fission of a small lipid vesicle (D ≈ 2 μm) from the bilayer into the aqueous droplet, reducing the bilayer's area and allowing it to approximate its original planar configuration. As the droplet continued to shrink, the bilayer buckled once more, revealing that the system will continue to cycle between Regimes 2 and 3 until the droplets have lost all water content. Vesicles were

dx.doi.org/10.1021/ja4019435 | J. Am. Chem. Soc. 2013, 135, 5545−5548

observed to eventually fuse to the interior of a monolayer interface, drawing lipids from it in a manner similar to the original bilayer. It was also observed that when one droplet was appreciably larger than its partner, the bilayer preferentially buckled and fissioned toward the larger droplet (see movies in Supporting Information). This directed fission could be caused by the initial curvature inherent to DIBs between droplets of disparate size[15b] and/or by asymmetric shape-change effects in the monolayers.

In conclusion, the evaporation-induced dynamic morphology of μDIBs was experimentally characterized. The droplets continually shrink around the preserved bilayer, forcing lipids from both monolayers to feed into the growing bilayer through a "conveyor-belt" effect. This results in the confinement and buckling of the bilayer, which fissions a vesicle at a critical radius of curvature and bending moment required for pinch-off. Evaporating DIBs offer unique dynamics between the coupled monolayer and bilayer interfaces, and the gradual deformation and rupture of the bilayer could be useful for modeling the mechanics of endo- and exocytosis in cells.

■ ASSOCIATED CONTENT

Supporting Information

Materials and methods, surface tension measurements, derivation of eq 2, and six movies of evaporating μDIBs. This material is available free of charge via the Internet at http://pubs.acs.org.

■ AUTHOR INFORMATION

Corresponding Author

colliercp@ornl.gov

Notes

The authors declare no competing financial interest.

■ ACKNOWLEDGMENTS

This research was conducted at the Center for Nanophase Materials Sciences, which is sponsored at Oak Ridge National Laboratory by the Scientific User Facilities Division, Office of Basic Energy Sciences, U.S. Department of Energy.

■ REFERENCES

(1) (a) Mueller, P.; Rudin, D. O.; Tien, H. T.; Wescott, W. C. *Nature* **1962**, *194*, 979. (b) Montal, M.; Mueller, P. *Proc. Natl. Acad. Sci. U.S.A.* **1972**, *69*, 3561.

(2) Rothman, J. E. *Nature* **1994**, *372*, 55.

(3) Walde, P.; Cosentino, K.; Engel, H.; Stano, P. *ChemBioChem* **2010**, *11*, 848.

(4) (a) Dobereiner, H. G.; Kas, J.; Noppl, D.; Sprenger, I.; Sackmann, E. *Biophys. J.* **1993**, *65*, 1396. (b) Menger, F. M.; Lee, S. J. *Langmuir* **1995**, *11*, 3685. (c) Staneva, G.; Angelova, M. I.; Koumanov, K. *Chem. Phys. Lipids* **2004**, *129*, 53. (d) Tanaka, T.; Sano, R.; Yamashita, Y.; Yamazaki, M. *Langmuir* **2004**, *20*, 9526. (e) Rawicz, W.; Smith, B. A.; McIntosh, T. J.; Simon, S. A.; Evans, E. *Biophys. J.* **2008**, *94*, 4725. (f) Yu, Y.; Vroman, J. A.; Bae, S. C.; Granick, S. *J. Am. Chem. Soc.* **2010**, *132*, 195. (g) Andes-Koback, M.; Keating, C. D. *J. Am. Chem. Soc.* **2011**, *133*, 9545. (h) Li, Y.; Kusumaatmaja, H.; Lipowsky, R.; Dimova, R. *J. Phys. Chem. B* **2012**, *116*, 1819.

(5) Seifert, U.; Berndl, K.; Lipowsky, R. *Phys. Rev. A* **1991**, *44*, 1182.

(6) McMahon, H. T.; Gallop, J. L. *Nature* **2005**, *438*, 590.

(7) Woo, H. J.; Wallqvist, A. *J. Phys. Chem. B* **2011**, *115*, 8122.

(8) Julicher, F.; Lipowsky, R. *Phys. Rev. E* **1996**, *53*, 2670.

(9) (a) Staykova, M.; Holmes, D. P.; Read, C.; Stone, H. A. *Proc. Natl. Acad. Sci. U.S.A.* **2011**, *108*, 9084. (b) Staykova, M.; Arroyo, M.; Rahimi, M.; Stone, H. A. *Phys. Rev. Lett.* **2013**, *110*, 028101.

(10) (a) Domanov, Y. A.; Kinnunen, P. K. J. *Biophys. J.* **2006**, *91*, 4427. (b) Thid, D.; Benkoski, J. J.; Svedhem, S.; Kasemo, B.; Gold, J. *Langmuir* **2007**, *23*, 5878. (c) Giger, K.; Lamberson, E. R.; Hovis, J. S. *Langmuir* **2009**, *25*, 71.

(11) Funakoshi, K.; Suzuki, H.; Takeuchi, S. *J. Am. Chem. Soc.* **2007**, *129*, 12608.

(12) (a) Suzuki, H.; Tabata, K.; Kato-Yamada, Y.; Noji, H.; Takeuchi, S. *Lab Chip* **2004**, *4*, 502. (b) Le Pioufle, B.; Suzuki, H.; Tabata, K. V.; Noji, H.; Takeuchi, S. *Anal. Chem.* **2008**, *80*, 328.

(13) (a) Funakoshi, K.; Suzuki, H.; Takeuchi, S. *Anal. Chem.* **2006**, *78*, 8169. (b) Holden, M. A.; Needham, D.; Bayley, H. *J. Am. Chem. Soc.* **2007**, *129*, 8650. (c) Hwang, W. L.; Holden, M. A.; White, S.; Bayley, H. *J. Am. Chem. Soc.* **2007**, *129*, 11854. (d) Villar, G.; Heron, A. J.; Bayley, H. *Nat. Nanotechnol.* **2011**, *6*, 803.

(14) (a) Hwang, W. L.; Chen, M.; Cronin, B.; Holden, M. A.; Bayley, H. *J. Am. Chem. Soc.* **2008**, *130*, 5878. (b) Syeda, R.; Holden, M. A.; Hwang, W. L.; Bayley, H. *J. Am. Chem. Soc.* **2008**, *130*, 15543. (c) Maglia, G.; Heron, A. J.; Hwang, W. L.; Holden, M. A.; Mikhailova, E.; Li, Q.; Cheley, S.; Bayley, H. *Nat. Nanotechnol.* **2009**, *4*, 437. (d) Sarles, S. A.; Leo, D. J. *Lab Chip* **2010**, *10*, 710. (e) Punnamaraju, S.; Steckl, A. J. *Langmuir* **2010**, *27*, 618. (f) Fischer, A.; Holden, M. A.; Pentelute, B. L.; Collier, R. J. *Proc. Natl. Acad. Sci. U.S.A.* **2012**, *108*, 16577. (g) Punnamaraju, S.; You, H.; Steckl, A. J. *Langmuir* **2012**, *28*, 7657.

(15) (a) Dixit, S. S.; Kim, H.; Vasilyev, A.; Eid, A.; Faris, G. W. *Langmuir* **2010**, *26*, 6193. (b) Dixit, S. S.; Pincus, A.; Guo, B.; Faris, G. W. *Langmuir* **2012**, *28*, 7442.

(16) Aghdaei, S.; Sandison, M. E.; Zagnoni, M.; Green, N. G.; Morgan, H. *Lab Chip* **2008**, *8*, 1617.

(17) (a) Poulos, J. L.; Nelson, W. C.; Jeon, T. J.; Kim, C. J.; Schmidt, J. J. *Appl. Phys. Lett.* **2009**, *95*, 013706. (b) Martel, A.; Cross, B. *Biomicrofluidics* **2012**, *6*, 012813.

(18) (a) Stanley, C. E.; Elvira, K. S.; Niu, X. Z.; Gee, A. D.; Ces, O.; Edel, J. B.; deMello, A. J. *Chem. Commun.* **2010**, *46*, 1620. (b) Elani, Y.; deMello, A. J.; Niu, X.; Ces, O. *Lab Chip* **2012**, *12*, 3514.

(19) Thiam, A. R.; Bremond, N.; Bibette, J. *Langmuir* **2012**, *28*, 6291.

(20) (a) Jung, S. Y.; Retterer, S. T.; Collier, C. P. *Lab Chip* **2010**, *10*, 3373. (b) Boreyko, J. B.; Mruetusatorn, P.; Retterer, S. T.; Collier, C. P. *Lab Chip* **2013**, *13*, 1295.

(21) (a) Jung, S. Y.; Retterer, S. T.; Collier, C. P. *Lab Chip* **2010**, *10*, 2688. (b) Collier, C. P.; Simpson, M. L. *Curr. Opin. Biotechnol.* **2011**, *22*, 516. (c) Lian, M.; Collier, C. P.; Doktycz, M. J.; Retterer, S. T. *Biomicrofluidics* **2012**, *6*, 044108.

(22) (a) Sackmann, E. *FEBS Lett.* **1994**, *346*, 3. (b) Lis, L. J.; McAlister, M.; Fuller, N.; Rand, R. P. *Biophys. J.* **1982**, *37*, 667.

(23) Paxson, A. T.; Varanasi, K. K. *Nat. Commun.* **2013**, *4*, 1492.

(24) Baoukina, S.; Monticelli, L.; Risselada, H. J.; Marrink, S. J.; Tieleman, D. P. *Proc. Natl. Acad. Sci. U.S.A.* **2008**, *105*, 10803.

(25) Solon, J.; Pecreaux, J.; Girard, P.; Faure, M. C.; Prost, J.; Bassereau, P. *Phys. Rev. Lett.* **2006**, *97*, 098103.

(26) Zhao, Y.; An, L.; Fang, J. *Nano Lett.* **2007**, *7*, 1360.

(27) (a) de Haas, K. H.; Blom, C.; van den Ende, D.; Duits, M. H. G.; Mellema, J. *Phys. Rev. E* **1997**, *56*, 7132. (b) Jonsson, P.; Beech, J. P.; Tegenfeldt, J. O.; Hook, F. *J. Am. Chem. Soc.* **2009**, *131*, 5294.

(28) Smith, K. A.; Uspal, W. E. *J. Chem. Phys.* **2007**, *126*, 075102.

(29) Lipowsky, R. *Nature* **1991**, *349*, 475.

(30) Taylor, G. I. *Proc. R. Soc. London A* **1934**, *146*, 0501.

(31) Liu, Y.; Jung, S. Y.; Collier, C. P. *Anal. Chem.* **2009**, *81*, 4922.